



Image Transformation With Lung Image Thresholding and Segmentation Method

Sahat Sonang S¹, Y. Yuhandri², Adil Setiawan³

¹Politeknik Bisnis Indonesia

²Universitas Putra Indonesia YPTK Padang

³Universitas Potensi Utama

¹sahatsonangstg@gmail.com, ²yuhandri@upiyptk.ac.id, ³adio165@gmail.com

Abstract

Image transformation is important to obtain and find certain information about an image that was not previously known, such as pixels, geometry, size, and color. Following this, this research aims to analyze image transformation in producing better values using threshold and segmentation methods. The segmentation process is carried out based on two color models, namely hue saturation value (HSV) and red green blue (RGB). The image data used in this study was the x-ray image of the lungs from www.fk.unair.ac.id, which is processed using the Matlab 2021a application to help the analysis process. On the results of the image segmentation analysis carried out in this case, the greater the HSV and RGB threshold values used in the image data, the better and clearer the segmentation of the detected image results. In other words, the size of the thresholding value generated greatly affects the quality, brightness, size, and color of the resulting image. The best lung X-ray image segmentation results were obtained when using the threshold values HSV = 0.9 and RGB = 9.

Keywords: transformation; image; threshold; segmentation; lung

1. Introduction

Image segmentation is a very important part of image processing, which is used to divide an image into two or more parts and process image partitions into several regions, not overlapping and homogeneous [1]. Image segmentation is a difficult problem in understanding image analysis and computer vision [2]. In image processing, the segmentation method is used to separate objects from the image background [3], [4]. Image segmentation is widely used in the medical world, including to identify organ pixels or lesions from medical images such as CT-scan or magnetic resonance imaging (MRI) [5], [6]. One of the segmentation methods that can be used is Thresholding [7], [8]. One of the image segmentation methods that can be used is thresholding, in which the processing is based on differences in the percentage of gray images. At the time of implementing image segmentation, a limit value is needed which is called the threshold value. Where if the image intensity value is greater than or equal to the threshold value, then it is changed to 1 (white color) but if the image intensity value is smaller than the threshold value then it is changed to 0 (white color). Thus the output image from thresholding is a binary image [9–11]. The segmentation process in images can be used in

several applications, although there are many variations of the method used, which have the same goal, namely obtaining a simple, useful representation of an image [12].

Various choices of methods that can be used in image segmentation, choosing the best method is very difficult because in determining the method used depends on the approach used as well as the features to be produced from the image [13], [14]. The segmentation process is closely related to image transformation because by using the segmentation method, the image will transform into another form so that it is different from the original image [15], [16]. In this paper, the process of image segmentation and transformation is both analyzed using the thresholding method, because the method can do it simultaneously [17], [18]. The use of thresholding methods has grown widely in solving many problems of image segmentation and transformation, which is evident from the studies that have been carried out [19], [20].

Research that proposes a new equilibrium optimization algorithm for multi-thresholding image segmentation problems. The result of this method can overcome large-scale problems with high efficiency and

outperform all other algorithms such as whale optimization algorithms, bat algorithms, sine-cosine algorithms, salp swarm algorithms, harris hawks algorithms, crow tracing algorithms, and particle swarm optimization in metrics used to evaluate segmented image quality for all threshold levels [21]. The research introduced the use of a new meta-heuristic algorithm called black widow optimization (BWO) to find the best threshold configuration using otsu or chalk as a goal function. To evaluate the performance and effectiveness of BWO-based methods, it was assessed using a variety of benchmark images, and compared to six well-known meta-heuristic algorithms including; whale optimization algorithm (WOA), equilibrium optimization (EO), gray wolf optimization (GWO), slap swarm algorithm (SSA), moth flame optimization (MFO), and sine cosine algorithm (SCA), slap swarm algorithm (SSA). The experimental results show that the proposed BWO-based method outperforms other algorithms in terms of fitness values as well as other performance measures. Statistical analysis shows that BWO-based methods achieve efficient and reliable results compared to other methods [22], [23].

Research that discusses color image segmentation uses adaptive hierarchical histogram thresholding. The experimental result show that this algorithm can obtain better segmentation results compared to histone-based techniques and roughness-index-based techniques with more efficient time complexity [24].

The purpose of this research is to find the intensity value or the gray level below it which is the background while above it is the foreground (object). One of the extensions of the proposed scheme is the minimum threshold (not the global minimum) of the proposed scheme's objective function [25], [26]. Research that discusses and proposes a rapid threshold segmentation method for froth images based on characteristic of pixel distribution. The size and distribution of the froth are important indexes in froth flotation.

Froth image segmentation has always been a problem in building floating models. In segmenting the froth image, the Otsu method is usually used to obtain a binary image for the classification of the froth image, this method can obtain satisfactory segmentation results. However, each level of grayness is required to calculate each variant between classes, so it takes longer on froth imagery with a large pixel count. To solve this problem, the threshold segmentation method is used [27].

Image segmentation is one of the most challenging problems in medical image analysis to differentiate between adjacent tissues in different parts of the body. In this context, suitable image pre-processing tools can improve the accuracy of results achieved by computer-assisted segmentation methods. By considering an image with a bimodal intensity distribution, the

thresholding technique image binarization can work well for segmentation of two classes with a bimodal histogram image, to overcome this limitation in order to automatically determine the optimal threshold according to the bimodal magnetic resonance (MR) image, by designing a framework intelligent image analysis in assisting doctors effectively in decision making.

Based on the related studies that have been explained, this study implements thresholding and segmentation methods to obtain threshold values from a pulmonary roentgen image. In this research, it consists of two parts of the process, namely: 1) The process of segmenting image transformation by combining two color segmentation results; 2) The segmentation process of Heu Saturation and value (HSV) is a process of separating objects by selecting colors according to the values of Heu, Saturation and Value (HSV).

2. Research Methods

2.1 Image Data

This study used data from lung X-ray images measuring 673 x 379 pixels obtained from the website www.fk.unair.ac.id.



Figure 1. Lung X-Ray Image

Chest X-ray or chest thorax X-ray (Figure 1) is a chest image that shows the image of the pocket, lung image, respiratory tract image, blood vessel canal, and lymph nodes. A chest X-ray or thoracic X-ray is an examination using electromagnetic wave radiation to display a picture of the inside of the chest. Through this examination, you can see the image of the spine and chest image, rib image, heart image, lung image, upper spine image, respiratory tract, blood vessels, and lymph nodes [28]. Reading or analyzing thoracic x-rays (chest x-rays) requires an understanding of the anatomy and physiology of the chest organs and an understanding of the limitations of radiological examination.

There are still many doctors, as well as the radiological part who made mistakes in the thoracic X-ray readings. According to the Indonesian doctor competency standard (SKDI) in 2012, the reading of thoracic X-ray results is categorized at level 4a where the explanation of the analysis results of photo X-rays can be done by general practitioners because they are equipped with clinical skills independently and without supervision.

2.2 Flowchart

The process of image transformation segmentation in this study is to combine two color segmentation results, namely based on HSV and RGB. The flow chart can be seen in Figure 2.

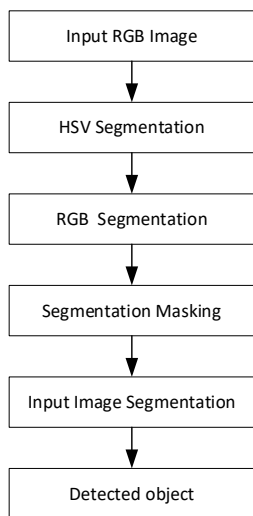


Figure 2. Process of Overall Segmentation Stages

Based on figure 2 above, shows the process of segmentation stages in combining 2 (two) color segmentations in the color input image data. In the next stage, the Hue, Saturation, and Value (HSV) image segmentation process is carried out, after this process is completed, the process is then carried out using Red Green Blue (RGB) segmentation. The results of these two segmentations are then used in forming masking segmentation which will be used in retrieving objects. The next stage is the segmentation on the input image so that the next stage of the selection process in determining the image can be detected.

The segmentation process of Hue, Saturation, and Value (HSV) is a process of separating objects by selecting colors according to the values of Hue, Saturation, and Value (HSV). The proximity of the visual process depicted by the human eye as well as distinguishing color perception well makes the HSV color model more often used than the RGB model. The HSV color space model is a transformation of an RGB color cube along a gray axis (diagonal axis of a combination of black and white dots), resulting in a conical color palette. Hue, Saturation, and Value in the HSV color system. The following is a description of the HSV channel: The Hue attribute is a pure color representation. The saturation attribute indicates the effect of white light affecting the degree of color dominance. The attribute value indicates the difference in brightness with pure color.

The process of segmenting the Hue, Saturation, and Value (HSV) and Red Green Blue (RGB) images can be seen in figure 3.

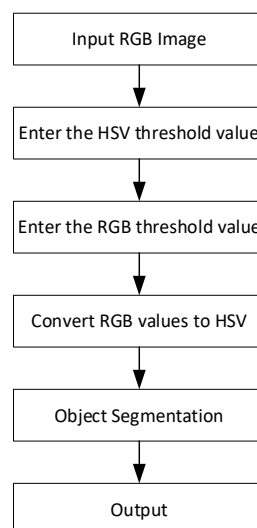


Figure 3. Stages of HSV and RGB Segmentation Process

Figure 3 shows the process of the Hue, Saturation, and Value (HSV) and Red Green Blue (RGB) segmentation stages. Initially, the RGB image is loaded. Then determine the Threshold Hue, Saturation, and Value (HSV) values with parameter values in Matlab 0.1, 0.2, 0.3, 0.4, 0.5, 0.6, 0.7, 0.8, and 0.9. The value of the Hue, Saturation, and Value (HSV) attributes is the value of the object to be detected. After that determine the Threshold Red Green Blue (RGB) value with parameter values in Matlab 1, 2, 3, 4, 5, 6, 7, 8, and 9. The next stage is the conversion of Red Green Blue (RGB) to Hue, Saturation, and Value (HSV) followed by object segmentation. Based on the parameter values that have been given to Hue, Saturation, and Value (HSV) and Red Green Blue (RGB), different final image results will appear.

3. Results and Discussions

The method used in this research is to build an evolutionary framework in image enhancement, automatic global thresholds, and segmentation. The framework used in the pre-processing resistance is MedGa. MedGa is an image enhancement method based on a genetic algorithm in increasing the threshold. The results obtained from this study quantitatively show that the use of MedGa as a pre-processing stage outperforms conventional image enhancement methods. The accuracy of bimodal magnetic resonance (MR) image segmentation is greatly improved making it especially suitable for clinical contexts requiring bimodal magnetic resonance (MR) image analysis and segmentation, which aims to provide useful insights in diagnosis. To obtain the threshold value, the calculation process is carried out. The first step that must be done is to make a histogram. From the histogram, it can be seen the number of pixels for each gray level. The gray level of the image is expressed by I to L. The I level starts from 1, namely pixel 0. For L, the maximum level

is 256 with a pixel value of 255. The threshold value to be searched for from a grayscale image is expressed by k . The value of k ranges from 0 to $L-1$, with a value of $L=256$ (the histogram symbol is P_i). So the probability of each pixel at level i is expressed by formula 1

$$P_i = \frac{n_i}{N} \quad (1)$$

P_i is the pixel probability i.e, n_i is the number of pixels with gray level I , and N is the the total number of pixels in the image.

Next look for the cumulative total value, cumulative average and global intensity. Formula 2 is for calculating the cumulative sum of $\omega(k)$, for $L = 0, 1, 2, \dots, L-1$.

$$\omega(k) = \sum_{i=0}^k P_i \quad (2)$$

Equation 3 is to calculate the cumulative mean of $\mu(k)$, for $L = 0, 1, 2, \dots, L-1$.

$$\mu(k) = \sum_{i=0}^k i \cdot P_i \quad (3)$$

Equation 4 is to calculate the global average intensity $\mu_T(k)$

$$\mu_T(k) = \sum_{i=0}^{L-1} i \cdot P_i \quad (4)$$

In equation 2, equation 3, and equation 4, the value of k represents the gray level at which each pixel range will be calculated. Next calculate the variance between classes. Equation 5 is for between class variance.

$$\sigma_B^2(k) = \frac{[\mu_T \omega(k) - \mu(k)]^2}{\omega(k)[1 - \omega(k)]} \quad (5)$$

The results of the calculation between class variance are sought for the maximum value. The largest value is used as the threshold or threshold value (k), with Equation 6

$$\sigma_B^2(k^*) = \max_{1 \leq x \leq L} \sigma_B^2(k) \quad (6)$$

$\omega(k)$ is the Cumulative Total, $u(k)$ is the Cumulative Average, $u_T(k)$ is the Global Intensity Averag, and σ_B^2 is the Threshold Value [9].

In general, the program thresholding algorithm used for the segmentation process in this study can be seen in the following pseudocode:

Algorithm THRESHOLDING

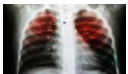
```
{ Clean the monitor/screen }
cls
{ Read the image file to be trained }
Img ← read('citra_paru.jpg')
write(Img)
{ Determine the HVS threshold value starting from 0.2;0.3;...;0.9}
Thres_HSV ← 0.9
{ Determine the HVS threshold value starting from 2; 3;...; 9}
Thres_RGB ← 9
{ Read pixel position }
```

```
P ← Read(gca,[])
{ Selecting the pixel position to be segmented by double clicking on the selected area }
P ← wait(P)
X ← round(P(1,1))
Y ← round(P(1,2))
{ assigns a reference color to the RGB space }
RGB1 ← Img(Y,X,:)
R ← RGB(:,1)
G ← RGB(:,2)
B ← RGB(:,3)
{ convert the reference pixel color }
HSV1 ← rgb2hsv(RGB1)
H12 ← HSV(:,1)
S12 ← HSV(:,2)
V12 ← HSV(:,3)
{ Image conversion to HSV and HCL color space }
citra_hsv1 ← rgb2hsv(Img)
[m,n,l] ← size(citra_hsv1)
{ Initialize the resulting image matrix }
cit_hasilHSV1(1:m,1:n,1:l) ← uint8(0)
cit_hasilRGB1(1:m,1:n,1:l) ← uint8(0)
for i ← 1:m
    for j ← 1:n
        { calculate the RGB color range }
        dR1 ← (abs(Img(i,j,1)-R))^2
        dG1 ← (abs(Img(i,j,2)-G))^2
        dB1 ← (abs(Img(i,j,3)-B))^2
        check1 ← sqrt(double(dR1+dG1+dB1))
        if (check1 <= Thres_RGB)
            cit_hasilRGB1(i,j,:) ← Img(i,j,:)
        end
        { Calculates the HSV color range }
        dH1 ← citra_hsv1(i,j,1)-H12
        S21 ← citra_hsv1(i,j,2)
        dV1 ← (citra_hsv1(i,j,3)-V12)^2
        Dcyl ← sqrt(double((dV1
        +(S12*S12)+(S21*S21)) - (2*S12*S21*cos(dH1))))
        if (Dcyl <= Thres_HSV)
            cit_hasilHSV1(i,j,:) ← Img(i,j,:)
        end
    end
end
{ display image results }
write(cit_hasilHSV1)
write(cit_hasilRGB1)
```

Based on the pseudocode, the threshold values for HSV images were generated and increased from 0.1 to 0.2, 0.3, 0.4, 0.5, 0.6, 0.7, 0.8, to 0.9, while the threshold values for RGB images were generated and increased from 1 to 2, 3, 4, 5, 6, 7, 8 to 9. For the comparison results of each image display based on the generated threshold value as shown in Table 1 to Table 9. The images presented in table 1 are different from the four. The selected image color in the red area which is the HSV result looks dominated by black and a few red color points, while the RGB results are still dominated

by black with more and thicker red than the HSV results. While the image color selected in the white area which is the result of HSV is clearer, the black and white colors forming a red color frame do not exist, while the RGB results for white, black, and red are quite clearly visible.

Table 1. Image Results with threshold values HSV=0.1 and threshold RGB=1

Image Color Selected	Original Image	HSV Result Image	RGB Result Image
Red Area			
White Area			

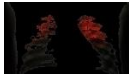
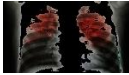
The imagery presented in table 2 differs from all four. The image color chosen in the red area which is the HSV result looks dominated by black and there is a red dot, while the RGB result is dominated by black with redder than the HSV result. While the image color chosen in the white area which is the HSV result is clearer black and white red colors are absent, while the RGB results of white, black, and red colors are quite clearly visible.

Table 2. Image Results with threshold values HSV=0.2 and threshold RGB=2

Image Color Selected	Original Image	HSV Result Image	RGB Result Image
Red Area			
White Area			

In table 3 the selected image color in the red area which is the result of HSV shows that the combination of black colors dominates but the red color is more visible than in the HSV results in table 2, while the RGB results are dominated by black with some red colors forming 2 stacks. While the color of the image selected in the white area which is the result of HSV is dominated by white and black with a hint of red, while the RGB results for black and red look quite clear, the white color is not clear.

Table 3. Image Results with threshold values HSV=0.3 and threshold RGB=3

Image Color Selected	Original Image	HSV Result Image	RGB Result Image
Red Area			
White Area			

In table 4 the selected image color in the red area which is the HSV result shows clearer black and red where black is more dominant, while the RGB results are dominated by black and red looks less bright. Meanwhile, the image color selected in the white area which is the result of HSV white and black is brighter and there are red spots, while the RGB results of black, red and white look faded.

Table 4. Image Results with threshold values HSV=0.4 and threshold RGB=4

Image Color Selected	Original Image	HSV Result Image	RGB Result Image
Red Area			
White Area			

In table 5 the selected image color in the red area which is the HSV result shows that the black color dominates more and the colors look brighter, while the RGB results are dominated by black but the white color is clearly visible enough. Meanwhile, the image color selected in the white area which is the HSV result of white and black looks brighter and the red spots are more clearly visible, while the RGB results for white, black, red and white look brighter.

Table 5. Image Results with threshold values HSV=0.5 and threshold RGB=5

Image Color Selected	Original Image	HSV Result Image	RGB Result Image
Red Area			
White Area			

In table 6 The image color selected in the red area which is the HSV result is very clearly visible the pattern image is black chest red brighter white color shows the chest frame, while the RGB result is dominated by black but the red color is bright enough to be located on the left and right chest and there is a fading black color. While the image color chosen on the white area which is the result of HSV white looks lighter, red fades and the black color is bright enough to cover red, while the RGB result is very bright white, the red color is bright enough so that it is clear the cavities on the black chest look bright.

In table 7 The image color selected in the red area which is the HSV result looks dominated by black in the end the cavity image is not visible but the red color is very clear on the image on the left and right chest, while the RGB result shows the black image still dominates but shows the image of the chest cavity, the red color looks

quite clear which forms the image on the left and right chest. While the image color chosen in the white area is the result of HSV visible very clearly the pattern image white color shows the chest cavity, red looks bright covering the red chest, while the RGB results show a brighter and clearer image, red looks bright, white very bright images image cavity black looks bright.

Table 6. Image Results with threshold values HSV=0.6 and threshold RGB=6

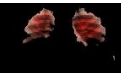
Image Color Selected	Original Image	HSV Result Image	RGB Result Image
Red Area			
White Area			

Table 7. Image Results with threshold values HSV=0.7 and threshold RGB=7

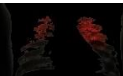
Image Color Selected	Original Image	HSV Result Image	RGB Result Image
Red Area			
White Area			

In table 8 the selected image color in the red area which is the result of HSV looks dominated by black and the image looks broken, the red color looks bright enough to form the image on the left and right chest cavities, and white color combines with red and white to form the pattern of spots, while the RGB results show that the black image still dominates but shows the image of the chest cavity fading, the red color looks faded which forms the image on the left and right chest. While the color of the image chosen in the white area is the result of the HSV, it is very clear that the image pattern is white, the white color shows the chest cavity, and the red color looks bright which combines with the white color, the red color covers part of the red color image, while the RGB results show a brighter and clearer image than HSV results.

Table 10. Qualitative Results of Testing

Threshold value HVS	RGB	Image Color Selected	HSV Result Image Value			RGB Result Image Value		
			Hue	Saturation	Value	Red	Green	Blue
0,1	1	Area Merah	0.4137	0.1032	0.0830	115.177	64.133	50.830
0,1	1	Area Putih	347.387	351.540	352.023	997.344	898.673	858.493
0,2	2	Area Merah	23.975	0.7075	0.56364	102.802	56.937	44.753
0,2	2	Area Putih	454.679	459.139	458.158	1.031.284	932.890	892.616
0,3	3	Area Merah	57.940	19.572	15.775	106.779	59.284	46.739
0,3	3	Area Putih	594.569	598.560	595.023	866.802	907.031	1.005.687
0,4	4	Area Merah	103.464	40.295	32.979	118.210	66.149	52.572
0,4	4	Area Putih	684.442	685.802	679.206	1.023.766	925.287	885.025
0,5	5	Area Merah	152.028	65.671	54.460	121.620	68.339	54.445
0,5	5	Area Putih	759.739	755.297	744.086	1.020.938	922.418	882.149
0,6	6	Area Merah	204.631	102.375	86.850	133.018	75.752	60.844
0,6	6	Area Putih	831.340	817.213	800.756	1.019.058	920.523	880.246
0,7	7	Area Merah	255.075	144.406	125.260	139.846	80.203	64.665

Table 8. Image Results with threshold values HSV=0.8 and threshold RGB=8

Image Color Selected	Original Image	HSV Result Image	RGB Result Image
Red Area			
White Area			

In table 9 The image color selected in the red area which is the result of HSV is very clearly visible and displays a clear image of the chest cavity that looks good red displays a bright and clear image, and the white color is very bright, as well as the black color is visible, while the RGB results show that black is very dominating the image, red color forms an image that looks quite clear and the presence of fading black color forms the image of the cavity on the chest. While the image color chosen in the white area is the result of HSV it is very clear that the pattern image is white showing the chest cavity, the red color looks bright which combines with the white color the image results are better than the overall test results, while the RGB results show a brighter and clearer image of all the test results from this image shows the best results.

Table 9. Image Results with threshold values HSV=0.9 and threshold RGB=9

Image Color Selected	Original Image	HSV Result Image	RGB Result Image
Red Area			
White Area			

Qualitative results of the tests carried out by changing the HVS threshold and RGB threshold values can be seen in table 10.

Threshold value		Image Color Selected	HSV Result Image Value		RGB Result Image Value			
HVS	RGB		Hue	Saturation	Value	Red	Green	Blue
0,7	7	Area Putih	886.393	861.451	840.527	1.038.862	940.519	900.208
0,8	8	Area Merah	793.165	690.911	665.100	147.198	85.605	69.391
0,8	8	Area Putih	946.950	906.909	880.282	1.039.090	940.744	900.432
0,9	9	Area Merah	1.046.108	947.601	910.098	144.437	83.564	67.593
0,9	9	Area Putih	1.011.822	946.905	913.250	1.034.134	935.747	895.442

In table 10, you can see the results of qualitative testing of images by changing the threshold values of HVS and RGB with the same image area. This result shows that changes in the HVS and RGB threshold values can affect image quality, where the greater the HVS and RGB threshold values used in the image data, the better and clearer the segmentation results are shown by changes in larger pixel values.

4. Conclusion

Based on the results of image segmentation analysis in this case, the greater the HSV and RGB threshold values used in the image data, the better and clearer the image segmentation results are detected. In other words, the size of the generated threshold value greatly affects the quality, brightness, size and color of the resulting image display. The best results of lung X-ray image segmentation when using threshold values HSV = 0.9 and RGB = 9.

Reference

- [1] X. Ma, W. Zhao, X. Hao, Y. Yang, and K. Yang, "Remote Sensing Image Registration with Adjustable Threshold and Variational Mixture Transformation," *IEEE Geosci. Remote Sens. Lett.*, vol. 17, no. 5, pp. 765–769, May 2020, doi: 10.1109/LGRS.2019.2936396.
- [2] Y. Fang, D. Yang, and J. Gan, "Image Segmentation Based on Superpixel Boundary Movement."
- [3] S. Song and T. Gao, "Research on image segmentation algorithm based on threshold," in *Proceedings - 2021 13th International Conference on Measuring Technology and Mechatronics Automation, ICMTMA 2021*, Jan. 2021, pp. 306–308. doi: 10.1109/ICMTMA52658.2021.00071.
- [4] L. Tong, "A dynamic-thresholding image segmentation algorithm for ceramic images based on Convolutional regression model," in *2021 IEEE 3rd International Conference on Communications, Information System and Computer Engineering, CISCE 2021*, May 2021, pp. 261–265. doi: 10.1109/CISCE52179.2021.9445994.
- [5] M. Alkhodari, O. Hassanin, and S. Dhou, "A Comparative Study of Meningioma Tumors Segmentation Methods from MR Images," Nov. 2020. doi: 10.1109/ICSPIS51252.2020.9340134.
- [6] IEEE Staff, *2018 Ural Symposium on Biomedical Engineering, Radioelectronics and Information Technology (USBEREIT)*. IEEE, 2018.
- [7] A. Kirthika, N. S. Madhava Raja, R. Sivakumar, and S. Arunmozhi, "Assesment of Tumor in Breast MRI using Kapur's Thresholding and Active Contour Segmentation," Jul. 2020. doi: 10.1109/ICSCAN49426.2020.9262402.
- [8] B. Khorram and M. Yazdi, "A New Optimized Thresholding Method Using Ant Colony Algorithm for MR Brain Image Segmentation," *J. Digit. Imaging*, vol. 32, no. 1, pp. 162–174, Feb. 2019, doi: 10.1007/s10278-018-0111-x.
- [9] JCT College of Engineering and Technology, IEEE Aerospace and Electronic Systems Society, and Institute of Electrical and Electronics Engineers, *ICISC 2018 : proceedings of the 2nd International Conference on Inventive Systems and Control (ICISC 2018) : 19-20 January 2018*.
- [10] D. heng Xie, M. Lu, Y. fang Xie, D. Liu, and X. Li, "A fast threshold segmentation method for froth image base on the pixel distribution characteristic," *PLoS One*, vol. 14, no. 1, Jan. 2019, doi: 10.1371/journal.pone.0210411.
- [11] E. H. Houssein, B. E. din Helmy, D. Oliva, A. A. Elngar, and H. Shaban, "A novel Black Widow Optimization algorithm for multilevel thresholding image segmentation," *Expert Syst. Appl.*, vol. 167, Apr. 2021, doi: 10.1016/j.eswa.2020.114159.
- [12] L. Yi, "A progressive image semantic segmentation method using recurrent neural network," in *2021 IEEE 6th International Conference on Intelligent Computing and Signal Processing, ICSP 2021*, Apr. 2021, pp. 765–768. doi: 10.1109/ICSP51882.2021.9408920.
- [13] M. Abdel-Basset, V. Chang, and R. Mohamed, "A novel equilibrium optimization algorithm for multi-thresholding image segmentation problems," *Neural Comput. Appl.*, vol. 33, no. 17, pp. 10685–10718, Sep. 2021, doi: 10.1007/s00521-020-04820-y.
- [14] Z. Yan, J. Zhang, Z. Yang, and J. Tang, "Kapur's Entropy for Underwater Multilevel Thresholding Image Segmentation Based on Whale Optimization Algorithm," *IEEE Access*, vol. 9, pp. 41294–41319, 2021, doi: 10.1109/ACCESS.2020.3005452.
- [15] T. H. Lee, L. T. Huang, P. Kuo, C. K. Wang, and J. I. Guo, "Focal-balanced attention u-net with dynamic thresholding by spatial regression for segmentation of aortic dissection in CT imagery," in *Proceedings - International Symposium on Biomedical Imaging*, Apr. 2021, vol. 2021-April, pp. 541–544. doi: 10.1109/ISBI48211.2021.9434028.
- [16] M. Hosein Hamian, A. Beikmohammadi, A. Ahmadi, and B. Nasersharif, "Semantic Segmentation of Autonomous Driving Images by the Combination of Deep Learning and Classical Segmentation," Mar. 2021. doi: 10.1109/CSICC52343.2021.9420573.
- [17] Vaigai College of Engineering and Institute of Electrical and Electronics Engineers, *Proceedings of the International Conference on Intelligent Computing and Control Systems (ICICCS 2020) : 13-15 May, 2020*.
- [18] B. Lei and J. Fan, "Image thresholding segmentation method based on minimum square rough entropy," *Appl. Soft Comput. J.*, vol. 84, Nov. 2019, doi: 10.1016/j.asoc.2019.105687.
- [19] T. Badriyah, N. Sakinah, I. Syarif, and D. R. Syarif, "Segmentation stroke objects based on CT scan image using thresholding method," in *Proceedings - 2019 1st International Conference on Smart Technology and Urban Development, STUD 2019*, Dec. 2019, pp. 61–65. doi: 10.1109/STUD49732.2019.9018825.
- [20] C. Patgiri and A. Ganguly, "Comparative study on different local adaptive thresholding techniques for detection of sickle cell anaemia from microscopic blood images," Dec. 2019. doi: 10.1109/INDICON47234.2019.9030304.
- [21] M. Li, L. Wang, S. Deng, and C. Zhou, "Color image segmentation using adaptive hierarchical-histogramthresholding," *PLoS One*, vol. 15, no. 1, Jan. 2020, doi: 10.1371/journal.pone.0226345.
- [22] M. H. Hesamian, W. Jia, X. He, and P. Kennedy, "Deep Learning Techniques for Medical Image Segmentation: Achievements and Challenges," *J. Digit. Imaging*, vol. 32, no. 4, pp. 582–596, Aug. 2019, doi: 10.1007/s10278-019-00227-x.
- [23] Dalian jiao tong da xue, Institute of Electrical and Electronics Engineers. Harbin Section, and Institute of Electrical and Electronics Engineers, *Proceedings of 2018 IEEE 3rd*

- International Conference on Cloud Computing and Internet of things : CCIOT 2018 : October 20-21, 2018, Dalian, China.*
- [24] L. Zhao, S. Zheng, W. Yang, H. Wei, and X. Huang, "An image thresholding approach based on Gaussian mixture model," *Pattern Anal. Appl.*, vol. 22, no. 1, pp. 75–88, Feb. 2019, doi: 10.1007/s10044-018-00769-w.
- [25] M. Dai, X. Leng, B. Xiong, and K. Ji, "An Efficient Water Segmentation Method for SAR Images," in *International Geoscience and Remote Sensing Symposium (IGARSS)*, Sep. 2020, pp. 1129–1132. doi: 10.1109/IGARSS39084.2020.9324113.
- [26] S. Ameer, "Image Thresholding Using the Complement Feature," *Am. J. Eng. Appl. Sci.*, vol. 13, no. 2, pp. 311–317, Feb. 2020, doi: 10.3844/ajeassp.2020.311.317.
- [27] M. El Bekkali, Institute of Electrical and Electronics Engineers. Morocco Section, F. École nationale des sciences appliquées, Jāmi‘at Sīdī Muḥammad ibn ‘Abd Allāh, and Institute of Electrical and Electronics Engineers, *The 7th Mediterranean Congress of Telecommunications 2019 : CMT 2019 : October 24-25, 2019, ENSA of Fez - Transmission and Information Processing Laboratory, USMBA University, Fez, Morocco.*
- [28] L. Rundo *et al.*, "A novel framework for MR image segmentation and quantification by using MedGA," *Comput. Methods Programs Biomed.*, vol. 176, pp. 159–172, Jul. 2019, doi: 10.1016/j.cmpb.2019.04.016.